Transport and Time Lag of Chlorofluorocarbon Gases in the Unsaturated Zone, Rabis Creek, Denmark

Peter Engesgaard,* Anker L. Højberg, Klaus Hinsby, Karsten H. Jensen, Troels Laier, Flemming Larsen, Eurybiades Busenberg, and L. Niel Plummer

ABSTRACT

Transport of chlorofluorocarbon (CFC) gases through the unsaturated zone to the water table is affected by gas diffusion, air–water exchange (solubility), sorption to the soil matrix, advective–dispersive transport in the water phase, and, in some cases, anaerobic degradation. In deep unsaturated zones, this may lead to a time lag between entry of gases at the land surface and recharge to groundwater. Data from a Danish field site were used to investigate how time lag is affected by variations in water content and to explore the use of simple analytical solutions to calculate time lag. Numerical simulations demonstrate that either degradation or sorption of CFC-11 takes place, whereas CFC-12 and CFC-113 are nonreactive. Water flow did not appreciably affect transport. An analytical solution for the period with a linear increase in atmospheric CFC concentrations (approximately early 1970s to early 1990s) was used to calculate CFC profiles and time lags. We compared the analytical results with numerical simulations. The time lags in the 15-m-deep unsaturated zone increase from 4.2 to between 5.2 and 6.1 yr and from 3.4 to 3.9 yr for CFC-11 and CFC-12, respectively, when simulations change from use of an exponential to a linear increase in atmospheric concentrations. The CFC concentrations at the water table before the early 1990s can be estimated by displacing the atmospheric input function by these fixed time lags. A sensitivity study demonstrates conditions under which a time lag in the unsaturated zone becomes important. The most critical parameter is the tortuosity coefficient. The analytical approach is valid for the low range of tortuosity coefficients (τ = 0.1–0.4) and unsaturated zones greater than approximately 20 m in thickness. In these cases the CFC distribution may still be from either the exponential or linear phase. In other cases, the use of numerical models, as described in our work and elsewhere, is an option.

Chlorofluorocarbons are volatile organic compounds used, for example, as aerosol propellants and refrigerants since the 1930s (Plummer and Busenberg, 1999) and now found in the subsurface because of the release to the atmosphere. There are numerous examples of the use of CFCs as tracers in groundwater studies, including studies of dating recharge water (Ekwurzel et al., 1994; Plummer et al., 2000), dating young groundwater (<50 yr) (Busenberg and Plummer, 1992; Oster et al., 1996; Plummer et al., 2001), groundwater flow and transport processes (Reilly et al., 1994; Cook et al., 1995, 1996; Szabo et al., 1996), flow and groundwater quality (Johnston et al., 1998; Böhlke and Denver, 1995), and groundwater–surface water interactions (Katz et al., 1995). A critical component in such analyses is the consideration of the transport and fate of the CFC tracers in the overlying unsaturated zone. For example, what are the CFC concentrations in recharge water and how long were the CFC gases in the unsaturated zone before reaching the groundwater system? The residence time of a CFC tracer in the unsaturated zone is also called the time lag (Cook and Solomon, 1995). An accurate estimate of the age of a groundwater sample also relies on an accurate estimate of the time lag.

For very shallow unsaturated zones of only a few meters thickness, diffusion and barometric pumping sufficiently mix the gases in the unsaturated zone so soil-gas CFC concentrations are similar to those in the troposphere. The input to the groundwater system is thus very close to the atmospheric changes in CFC concentrations. This simple approach often has been used for dating groundwater, where the concentrations measured in groundwater are used directly together with the atmospheric concentrations to estimate the time of recharge, thus neglecting any time lag of the CFCs in the unsaturated zone.

In deeper unsaturated zones the time lag can be important, and various processes affecting CFC transport become important. Gas diffusion and air–water exchange (solubility) are especially important in controlling the migration and attenuation rate. Both processes are a function of the water content and, thus, seasonal and year-to-year changes in infiltration and depth to the water table. Cook and Solomon (1995) investigated numerically the conditions under which the time lag of CFCs in the unsaturated zone is of importance by examining the relative effects of various soil parameters on the distribution of gases in the unsaturated zone. Busenberg and Plummer (2000) used the same model as Cook and Solomon (1995) to study lag times of SF_6 in unsaturated zones and found that the lag times of SF_6 are smaller than for CFCs because of its low solubility. Oster et al. (1996) measured 57 profiles of both CFC-11 and CFC-12 in a 4.5-m-thick unsaturated zone in a forest soil in Germany. A clear damping of the annual changes in CFC atmospheric concentrations were found with a relaxation time (time lag) of 30 d for 4 m. Weeks et al. (1982) used analytical and numerical transport models to simulate the observed distribution of CFC-11 and CFC-12 in a >50-m-deep unsaturated zone. The analytical model was a pure diffusion model, whereas the nu-

P. Engesgaard and K.H. Jensen, Geological Institute, Univ. of Copenhagen, Øster Voldgade 10, 1350 Copenhagen K, Denmark; A.L. Højberg, K. Hinsby, and T. Laier, Geological Survey of Denmark and Greenland, Øster Voldgade 10, 1350 Copenhagen K, Denmark; F. Larsen, Environment and Resources, Technical Univ. of Denmark, Building 204, 2800 Lyngby, Denmark; E. Busenberg and L.N. Plummer, USGS, 12201 Sunrise Valley Drive, Reston, VA 20192, USA. Received 4 July 2003. Original Research Paper. *Corresponding author (pe@geol.ku.dk).

Published in Vadose Zone Journal 3:1249–1261 (2004).

677 S. Segoe Rd., Madison, WI 53711 USA

Abbreviations: CFC, chlorofluorocarbon; GC, gas chromatography; GEUS, Geological Survey of Denmark and Greenland.

merical model also included advective transport because of the downward movement of the water table caused by increased pumping in the aquifer below. Weeks et al. (1982) were able to demonstrate that the procedures for estimating tortuosity (and thus also gaseous diffusion in soils) developed from theoretical considerations or laboratory techniques apply for field conditions as well. Busenberg et al. (1993) found that soil gas concentrations from two multilevel piezometers in a 46-m-deep unsaturated zone of sedimentary and basalt deposits could be explained by diffusion theory. Using the same model as Weeks et al. (1982) they were able to fit the tortuosity coefficients for the sedimentary and basalt deposits to CFC-11 and CFC-12 profiles. Severinghaus et al. (1997) measured CFC-11, CFC-12, and CFC-113 profiles in relatively dry and deep (60 m) unsaturated zones in sand dunes. A diffusion transport model simulated the profiles very well. The reported mean age of air (time lag) was 10 yr, and diffusion was found to be much more important than advection. Recently, transport of CFC gases in deep unsaturated fractured systems was investigated to study recharge mechanisms in a regional aquifer (Plummer et al., 2000) and chemical and physical processes at Yucca Mountain, Nevada, USA (Thorstenson et al., 1998).

The main objective of this work has been to simulate the historical input of CFC-11, CFC-12, and CFC-113 to groundwater at the Rabis Creek field site in Denmark. Observations of gas profiles in the 16-m-thick unsaturated zone are used for investigating the important physical-chemical processes affecting transport. In contrast to previous investigations, we explore the effect of nonsteady flow. As an outcome of the work, we also present a new analytical solution for predicting the distribution of CFCs in the soil and the historical input of CFCs to groundwater. Hinsby et al. (unpublished data, 2004) used groundwater input functions to investigate CFC transport and degradation in the underlying aquifer.

MATERIALS AND METHODS

Site Description

The site is situated just outside the main stationary line of the last glaciation (Weichsel/Wisconsin) in Rabis Creek, Denmark. Mean annual precipitation and groundwater recharge are 710 mm yr^{-1} (Andersen and Sevel, 1974) and 439 mm yr^{-1} (Engesgaard et al., 1996), respectively. The aquifer is unconfined, and the water table fluctuates <1 m annually at a depth of approximately 16 m below the surface. The subsurface hydrogeology consists of fairly homogeneous sandy deposits (Olsen et al., 1993) and can be regarded as a porous medium with no fracture flow. Postma et al. (1991) found O_2 to a depth of more than 10 m below the water table.

Field Investigations

Profiles of the CFC gases were from a single well. Sixteen 6-mm copper tube soil gas samplers with an approximately 50-mm screened section at the end were installed at intervals of 1 m from the surface to the water table. The copper tubes were attached to the outside of a 63-mm-diameter piezometer with a 2-m screen at the end. The piezometer with the copper tube soil gas samplers then was placed through a hollow auger stem that was augered down to just below the water table. Fine- to medium-grained quartz sand was used as gravel pack around the screened intervals, and a mixture of quartz sand and silt was used as low-permeability plugs to reduce the gas-permeability between the samplers. The copper tubes were equipped with fittings at the upper end for a convenient and air-tight connection to the CFC sampler. After installation, the copper tubes were purged simultaneously for 10 min by means of a small soil gas pump connected to a manifold. The installation then was left for one-half year before the first sampling was performed in September 1995.

At the time of sampling, the copper tubes were connected to the CFC sampler and the soil gases then were pumped through the borosilicate sampling ampoules by means of a small soil gas pump. At least three (3–10) copper tube volumes were flushed through the sample ampoule before the soil gas sample was taken by fusing the ampoule with a small torch for an air-tight seal. The ampoules were taken to the laboratory at the Geological Survey of Denmark and Greenland (GEUS) and transferred to the gas chromatograph and analyzed for CFC-11, CFC-12, and CFC-113 as described by Busenberg and Plummer (1992). A second set of samples was taken in June 1996 and analyzed at the USGS Chlorofluorocarbon Laboratory in Reston, VA. The CFCs were measured using purge-and-trap gas chromatography (GC). The CFCs were trapped at −30°C on a short Porasil C-Porapak T trap. The CFCs were released by heating the trap at 100°C and separated with a 3 by 3.13 mm o.d. stainless-steel column packed with Porasil C. The N_2 carrier gas flow was 40 cm^3 min^{-2}. The GC oven temperature was maintained at 70°C, and the CFCs were quantified with an electron capture detector held at 290°C (Busenberg and Plummer, 1992). During the second sampling, the soil gas samplers and sampling ampoules were purged exactly three times with a 50-mL syringe before sample collection.

An approximately 14-m-long sediment core was analyzed for its organic content (f_{oc}), water content (θ_w), and total porosity (θ). The core was subdivided into 56 subsamples. Each subsample was classified according to grain size. Parts of each subsample from the same classification (five in total) then were pooled and f_{oc} was measured, thus yielding average values of the organic content for each classification. The water content and porosity were measured for each of the 56 subsamples giving a vertical spatial distribution of the porosity and, at the time of sampling, of the water content.

THEORY

CFC Transport in the Unsaturated Zone

Gas transport is distinctly different for fractured and nonfractured media. For example, in a numerical study by Nilson et al. (1991), barometric transport rates were two orders of magnitude greater than transport by molecular diffusion. This difference is due to the highly increased flow rate through the fractures. Plummer et al. (2000) found evidence of barometric pumping in fractured basalt by observing high CFC concentrations at the water table. These were inconsistent with measured low tritium concentrations, indicating that the CFC gases were transported rapidly through fractures.

The 16-m-thick unsaturated zone at Rabis Creek is a homogeneous porous, nonfractured media. The primary mechanisms affecting transport of CFCs in an aerobic unsaturated zone is shown in Fig. 1 (Plummer and Busenberg, 1999). Gas transport in a variably saturated soil takes place as a combination of advective and diffusive–dispersive processes in both air and water. The water content changes over the season and diffusion in air and advective transport in both phases are sensitive

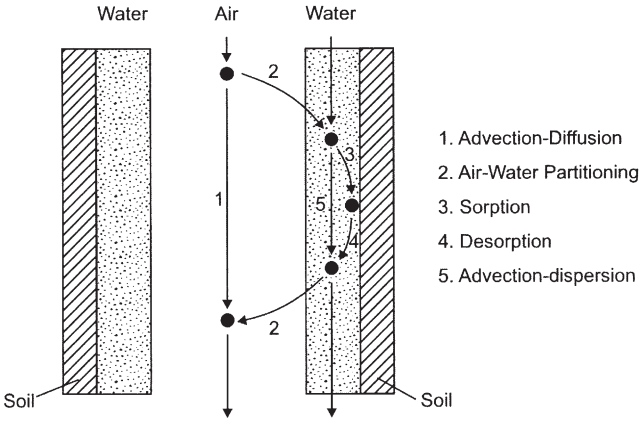

Fig. 1. Physical and chemical processes affecting CFC transport in the unsaturated zone.

to the water content (Cook and Solomon, 1995). The simulated average yearly infiltration at the site ranges from 266 to 623 mm yr^{-1} (see Water Content in Results below). A high water content, which may occur close to the soil surface under periods of infiltration and close to the water table, leads to reduced transport by gas diffusion by decreasing the effective area for diffusive flow and connectivity of gas-filled pores. However, at the same time, advective–dispersive transport in the water phase increases. Advective transport in the air phase also may occur as a result of variations in barometric pressure, wind blowing across the surface, temperature gradients, water infiltration and redistribution, and a moving water table. Weeks et al. (1982) and Kimball and Lemon (1972) found that many of these mechanisms contributed little to advective transport at depths of more than 1 m below the soil surface. On the other hand, the analysis by Massmann and Farrier (1992) suggested that gas can migrate several meters into the unsaturated zone by advective transport caused by atmospheric pressure fluctuations.

Diffusional transport in the gas phase generally is a rapid transport mechanism and typically faster than transport of CFCs in the water phase. Nielsen and Ørbeck (1995) found on the basis of air–water exchange models of Schwarzenbach et al. (1993) that the total transport times of CFC-11 and CFC-12 in air and water boundary layers (0.1–1 and 0.005–0.05 cm in thickness, respectively) are <6 min. Rapid exchange at the air–water surface (phase transfer), thus, can have a retarding effect on CFC transport.

Chlorofluorocarbon sorption–desorption may be controlled by kinetics with a time scale much longer than for air–water exchange. Little is known about CFC sorption. In the following we assume that sorption is an equilibrium process. Generally, it can be assumed that degradation of CFCs only occur in anaerobic environments (Plummer and Busenberg, 1999). There are only a few small-scale studies that demonstrate the onset of degradation with a change in redox environment. For example, Cook et al. (1995) found a significant decrease in CFC-11 concentration coincided with a decrease in O_2 concentration to below 0.5 mg L^{-1}. They estimated first-order degradation rates to 0.2 to 1.6 yr^{-1}. Happell et al. (2003) observed that CFC-11, CFC-12, and CFC-113 disappeared with a significant increase in methane concentration, which they attributed to the activity of methanogenic bacterial degradation of the CFC gases. The decrease or increase in solute concentration of different redox environment indicators may therefore point to the presence of degradation. Anaerobic microenvironments where degradation occurs may exist in the unsaturated zone, although the bulk part will remain aerobic without any degradation. First-order degradation is included in the model because detectable methane concentrations in the lower part of the unsaturated zone were observed.

Transport in the Water Phase

Transport of CFCs in the water phase of a variably saturated porous media can be described by

$$\frac{\partial}{\partial t}\left(R\rho_w\theta_w c_w\right) = \frac{\partial}{\partial z}\left(\rho_w\theta_w D_w\frac{\partial c_w}{\partial z} - \rho_w q_w c_w\right) - \lambda R\rho_w\theta_w c_w - \left(\frac{\partial c_a}{\partial t}\right)exch \quad [1]$$

where θ_w is the volumetric water content, ρ_w is the water density, c_w is the concentration of gas dissolved in water, c_a is the concentration of gas in the air, D_w is the dispersion coefficient, q_w is the Darcy flux, t is time, and z is depth oriented positive downwards. The dispersion coefficient is given by $D_w = \alpha_L v_w$, where α_L is the longitudinal dispersivity and v_w is the pore water velocity given as q_w/θ_w. In Eq. [1], it is assumed that the CFC can be affected by linear sorption (R) and first-order decay (λ). Sorption is modeled by the retardation factor $R = 1 + \rho_b/(\rho_w\theta_w)K_d$, where K_d is the solid–water distribution coefficient and ρ_b is the bulk density of the media. First-order degradation may be specified as a function of depth. The last term on the right-hand side of Eq. [1] accounts for the mass exchange between the water and air phases.

The solution to Eq. [1] was based on steady or nonsteady simulations of the flow field. A numerical code was used to solve the Richards equation for one-dimensional nonsteady flow based on local climatic information. The same unsaturated flow code was used by Engesgaard et al. (1996) to predict the average recharge from 1961 to 1970 at the same field site.

Transport in the Air Phase

Advective transport due to volumetric displacement, for example, from infiltration, is the only advective gas transport process included in the numerical code. Advective transport in air is approximated, as a complementary part of unsaturated water flow as the water- and gas-filled pore volumes must equal the total porosity. Assuming that air is incompressible and that the water table constitutes an impermeable boundary, advective transport in the numerical cell located just above the water table is calculated from the volumetric changes in water and air from one time step to the next. If the air volume increases, gas is transported into the cell from the cell above and vice versa for a decreasing air volume. Advective transport then can be calculated from the water table to the soil surface by keeping track of the volumetric changes and gas transport from the underlying cell. Using this procedure, a potentially important mechanism of advective gas transport is considered and a CFC mass balance over the two phases in the system is obtained. Variations in barometric pressure were not included in the simulations, but this mechanism was assumed to cause complete mixing of soil air in the upper 1 m. The CFC soil transport simulations were thus performed from 1 m below the soil surface giving a total length of 15 m unsaturated soil column.

The net transport of gas can be described by

$$\frac{\partial}{\partial t}(\theta_a c_a) = \frac{\partial}{\partial z}\left(\theta_a D_a\frac{\partial c_a}{\partial z} - q_a c_a\right) - \left(\frac{\partial c_w}{\partial t}\right)exch \quad [2]$$

where θ_a is the volumetric air content; $D_a = \tau D_{CFC}$ is the effective gas diffusion coefficient, where τ is the tortuosity of the porous media and D_{CFC} is the self-diffusion coefficient for the CFC gas into atmospheric air; and q_a is the advective flux of air as discussed above. The last term on the right-hand side

accounts for the mass exchange between the air and water phases. No sorption occurs in the air phase as all the solids are assumed to be fully surrounded by water. No degradation is assumed to take place in the air phase.

Air–Water Exchange

Assuming equilibrium exchange of CFC between the air and water phases, the relation between the air and water CFC concentrations can be expressed by Henry's Law as

$$c_w = K_{wa} c_a \quad [3]$$

where K_{wa} is the water–air partitioning coefficient, or Henry's constant, that is a function of temperature and salinity and can be calculated from equations provided by Warner and Weiss (1985) and Bu and Warner (1995).

Numerical and Analytical Solutions

Equations [1] and [2] are coupled through the water–air exchange term that can be computed from Eq. [3]. Both [1] and [2] were solved using a finite difference discretization and the coupled system of equations was solved with an Iterative Operator Splitting technique (Steefel and MacQuarrie, 1996).

There were no meteorological data available for the site before 1961. To estimate initial 1961 soil CFC concentrations, the mean water content and mean water flux for the period 1961 to 1996 was calculated and used as input in a CFC transport simulation based on steady flow from the start of atmospheric CFC release (1940–1950) to 1961. The upper boundary condition is that of specified concentration with the concentration in the air phase equal to the atmospheric concentration. The upper boundary condition for the concentration in water then is $c_w\,(z = 1m,t) = c_a K_{wa}$. The lower boundary condition, at the water table, is assumed to be in the form of a zero-gradient in concentration, or $(\partial c_a/\partial z)(z = L,t) = (\partial c_w/\partial z)(z = L,t) = 0$, where L is the total length of the soil profile. For the air phase, this implies a zero-flux boundary (impermeable), and for the water phase a pure advective flux boundary (no dispersion).

A spatial discretization step of 0.1 m was used in all simulations, resulting in 151 node points over the 15-m-deep profile. The simple procedure to calculate the advective component in air, q_a, was affected by numerical oscillations if a time step too large was used. A time step of 1 d was used, matching the frequency with which climatic input data were available. No oscillations were found using this time step, and simulations using a time step of 1 h gave almost identical results. If the advective component was not included, small oscillations were seen simply because mass was not conserved during a time step when the simulated nodal water content changed.

If degradation is neglected (typical in unsaturated zones), then transport of CFC for steady water flow can be described by adding Eq. [1] and [2], averaging all parameters, using Eq. [3] and the definition of the retardation coefficient, yielding

$$\theta^* \frac{\partial c_a}{\partial t} = D^* \frac{\partial^2 c_a}{\partial z^2} - q^* \frac{\partial c_a}{\partial z} \quad [4]$$

where θ^*, D^*, and q^* are the average volumetric air content, bulk diffusion coefficient, and advective flux of air, respectively, defined by

$$\theta^* = (\theta - \bar{\theta}_w) + \rho_w \bar{\theta}_w K_{wa} + \rho_b K_d K_{wa} \quad [5]$$

$$D^* = (\theta - \bar{\theta}_w)\tau D_{CFC} + \alpha_L \rho_w \bar{q}_w K_{wa} \quad [6]$$

$$q^* = \bar{q}_a + \rho_w \bar{q}_w K_{wa} \quad [7]$$

where $\bar{\theta}_w$, $\bar{q}_w$, and $\bar{q}_a$ are the mean water content, mean Darcy flux, and mean advective flux of air. Equations [4] and [5] through [7] are identical to the ones solved by Cook and Solomon (1995) in their steady flow analysis with no degradation and $\bar{q}_a = 0$.

For a system controlled by diffusion (neglecting advective flow of gas and water, $q_a = q_w = 0$) Weeks et al. (1982) and Cook and Solomon (1995) adapted an analytical solution from Carslaw and Jaeger (1959) to Eq. [4] using an upper boundary condition of exponentially increasing atmospheric concentration. Cook and Solomon (1995) used the analytical solution to define the time lag as the time it takes a CFC gas to move through the unsaturated zone. The time lag to an arbitrary depth is thus found from the relation

$$c_a(z, t) = c_0 \exp[k_e(t - t_L^e)] \quad [8]$$

where t_L^e is the time lag for the exponential phase, k_e is the rate of exponential increase in the atmospheric CFC function, and c_0 is the initial concentration. By setting the depth to L, the following is obtained (Cook and Solomon, 1995)

$$t_L^e = \frac{\ln\left[\cosh\left(L\sqrt{\frac{k_e\theta^*}{D^*}}\right)\right]}{k_e} \quad [9]$$

Equation [9] only is valid after a certain time has elapsed since initial conditions (terms dropped in original solution).

The atmospheric input function has a linear increase since the early 1970s to approximately the early 1990s for CFC-11 and CFC-12, and a much shorter period with a linear increase from 1985 to 1990 for CFC-113 (see below). Equation [9] is not necessarily valid for CFC profiles measured during the mid 1990s, such as in this study, and an analytical solution must, therefore, be based on a linear increase at the top boundary. Carslaw and Jaeger (1959) provided an analytical solution for the case of linear increase in atmospheric concentrations and zero initial concentrations as

$$c_a(z, t) = k_1 t + \frac{k_1 \theta^* z(z - 2L)}{2D^*} \quad [10]$$

where k_1 is the rate of linear increase in the CFC atmospheric input functions. Here, $z = 0$ also is at the soil surface and positive downwards. As in Eq. [9], second-order terms have been dropped in Eq. [10], and the solution only is valid after a certain period has elapsed since initial conditions. The solution assumes the concentration at the boundary starts at zero and that the initial concentrations are zero. An initial concentration of zero is not the case because the linear increase in atmospheric concentrations starts in the early 1970s. However, because a solution for large t is adapted, sufficiently long after the initial time, the effect of the initial concentrations can be neglected. Thus, the linear growth period can be assumed to start earlier than the 1970s. As an example, consider CFC-11, with an approximate linear growth rate after 1975 of $k_1 = 9.3$ pptv yr^{-1}. Since the CFC-11 concentration was approximately 115 pptv in 1975 (Fig. 2), it can be assumed, when using Eq. [10], that the atmospheric and initial concentration was zero in approximately $t_0 = 1962$. Therefore, time in Eq. [10] is relative to t_0, or

$$c_a(z, t) = k_1 (t - t_0) + \frac{k_1 \theta^* z(z - 2L)}{2D^*} \quad [11]$$

Following Cook and Solomon (1995) the time lag is defined as

$$c_a(z, t) = k_1 (t - t_0 - t_L^l) \quad [12]$$

where t_L^l is the time lag in the linear phase. Substituting Eq.

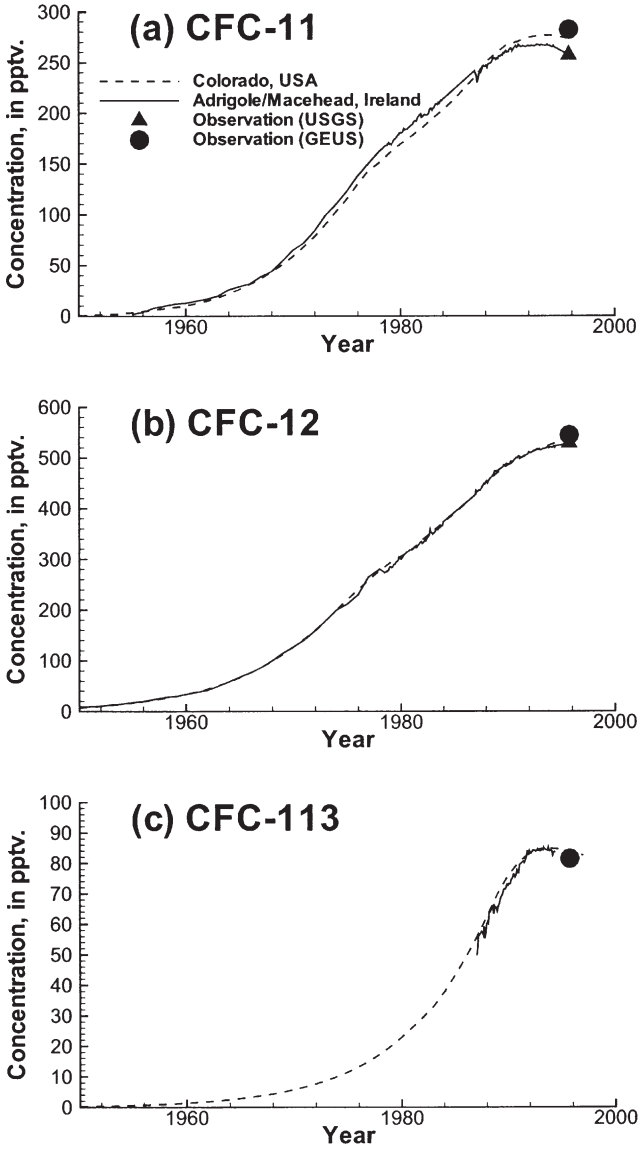

Fig. 2. Measured and reconstructed (a) CFC-11, (b) CFC-12, and (c) CFC-113 concentration curves for the atmosphere at monitoring stations in Ireland (solid line) and USA (dashed line). Two different measurements of the atmospheric CFC concentrations at the Rabis Creek study site are included.

[12] into Eq. [11] gives the time lag for the linear phase for any distance z below the soil surface:

$$t_L^l = \frac{\theta^* z(2L - z)}{2D^*} \quad [13]$$

The time lag at the water table ($z = L$) is

$$t_L^l = \frac{\theta^* L^2}{2D^*} = \frac{L^2}{2D_e} \quad [14]$$

where D_e is an effective diffusion coefficient. Equation [14] is a measure of the time scale for diffusion over the depth of the unsaturated zone.

DATA

Atmospheric Input Functions

Two atmospheric CFC concentration input functions were evaluated, one from USA and one from Europe. The applied North American atmosphere input function is from Niwot Ridge, Colorado (multi-sampler mixed continental air), typically used for groundwater dating in North America. The data from Niwot Ridge is part of a program run by the National Oceanic and Atmospheric Administration (NOAA)/Climate Monitoring and Diagnostics Laboratory (CMDL) in Boulder, CO (http://www.cmdl.noaa.gov/). The European atmosphere input function is from Western Europe (Ireland/N. Atlantic air), which is the long-term station closest to Denmark. To extend the monitored CFCs as far back in time as possible, the input function from Ireland was established by combining measurements from two stations. The monitoring station at Agricole, Ireland, operating from 1978 to 1983, was replaced in 1987 by a new station at Mace Head, Ireland. The Mace Head station is part of the ALE/GAGE/AGAGE global network (Prinn et al., 2000), whereas the pre-1980 curve was calculated from CFC production and release data of AFEAS (Alternative Fluorocarbons Environmental Acceptability Study, http://afeas.org) and was normalized to Niwot Ridge air. Similarly, the CFC-113 data are consistent with the recently revised AFEAS production and release data for CFC-113.

The three atmospheric CFC functions at the two sites are shown in Fig. 2. The increases in CFC-11 and CFC-12 concentrations are roughly exponential from the time of initial release to the early to mid 1970s. For CFC-113, the exponential growth period continues to the mid 1980s. Following the exponential period is a period of an approximately linear increase until the late 1980s to early 1990s, where CFC-11 and CFC-113 concentrations level off and recently decline. The atmospheric concentrations measured at the two locations were almost identical for CFC-12 and CFC-113. However, some differences for CFC-11 are found, especially for post-1985 concentrations. Although the CFC concentrations measured at unpolluted sites show little variation between monitoring stations on the northern hemisphere, Oster et al. (1996) found significant differences in local atmospheric CFC concentrations at four sites in geographically diverse regions in Germany and Switzerland. They showed that the concentrations of CFC-11 and CFC-12 increased with closer proximity to urban (industrialized) regions. At the Rabis Creek site no significant local sources were expected.

Only a few observations of atmospheric CFC concentrations are available at the Rabis Creek field site and in Denmark in general. The atmospheric CFC curves are compared with the few atmosphere measurements at Rabis Creek in Fig. 2. The measurements by GEUS consistently are higher than those by USGS, for CFC-11, with up to a 10% difference. Even when disregarding these analytical differences, it is not possible from these few measurements to decide which input function is the most appropriate to use at Rabis Creek. To quantify the sensitivity to the choice of atmospheric input function, the CFC distributions in the unsaturated zone were simulated with both input functions and compared with the observations from the multilevel samplers. The results showed that the simulations based on the Niwot Ridge curves gave the best fit to the observed data. Therefore the Niwot Ridge curves were used as input functions in the following analyses of CFC transport in the subsurface.

Climatic Data

Daily values of precipitation, potential evapotranspiration, and temperature collected at a nearby meteorological station were available. The same data were used by Engesgaard et al. (1996) to study tritium transport in the unsaturated zone at Rabis Creek.

Table 1. Physicochemical properties of CFC gases.†

CFC gas	D_{CFC}	K_w	K_{oc}
	$m^2\ d^{-1}$	$cm^3\ g^{-1}$	$g\ g^{-1}$
CFC-11	0.71	0.55	100
CFC-12	0.77	0.14	235
CFC-113	0.63	0.17	175

† D_{CFC} values for CFC-11 and CFC-12 are from Weeks et al. (1982) corrected to 8°C. D_{CFC} value for CFC-113 is taken directly from Cook and Solomon (1995) (uncorrected). K_w values are computed from Warner and Weiss (1985) (CFC-11 and CFC-12) and Bu and Warner (1995) (CFC-113) at 8°C. K_{oc} values are from Cook et al. (1995) at 25°C.

Physical and Chemical Parameters for Soil and CFC Gases

Some of the main physicochemical parameters for the CFC gases are given in Table 1. D_{CFC} values for CFC-11 and CFC-12 were taken from Weeks et al. (1982) and corrected to the ambient groundwater temperature of 8°C using the approximation $D_1/D_2 = (T_1/T_2)^m$, where D_i and T_i are the diffusion coefficient and temperature, respectively, and m was taken as 1.75 (Thomas, 1982).

The temporal and depth-dependent water content, θ_w, and flux of water, q_w, in Eq. [1] were obtained by solving the Richards equation, as explained above. Hydraulic properties for the sandy soil at the study site were not measured. Instead, measured properties for similar Danish coarse sand were specified. The soil was chosen so that the numerical simulations gave approximately the same mean water content as observed. A cubic spline function was fitted to measured retention data in the range from wilting point to porosity. Changes in unsaturated hydraulic conductivity with θ_w were predicted using a power function. The flow code was used to predict the variations in θ_w and q_w for 1961 through 1996.

The only unknowns in Eq. [1] through [3] are τ, K_d, λ, and α_L. Both tortuosity and sorption will have a retarding effect on CFC gas transport, and various combinations of the two can fit a CFC profile (Weeks et al., 1982). Both are regarded as fitting parameters. Based on measured values for f_{oc}, a theoretical distribution coefficient can be calculated from the relation $K_d = f_{oc}K_{oc}\rho_w$, where K_{oc} is the water–organic C partition coefficient (Table 1). This relation is derived for sorbing of nonpolar chemicals to aquifer material with $f_{oc} > 0.1\%$. Although the CFCs are not strictly nonpolar chemicals, they have been observed to act as such with respect to sorption (Ciccioli et al., 1980). For the soil at this site, Nielsen and Ørbeck (1995) measured a value of f_{oc} in the range of 0.005 to 0.014% below depths of 0.09 m and 0.129% for the top 0.09 m, representing an upper organic-rich layer. The depth-averaged f_{oc} value for the profile below 0.09 m is 0.008%. Theoretical K_d values of 0.008, 0.019, and 0.014 g g^{-1} for CFC-11, CFC-12, and CFC-113, respectively, can be calculated, although f_{oc} is <0.1% and the above relation is, thus, not strictly applicable. Given the low organic C content we anticipate little retardation and a starting assumption is K_d = 0 for all CFC gases.

Small amounts of methane (0.015% [v/v]) were detected in the lower 4 m of the profile, indicating that degradation in microenvironments is a possibility. Specifying a first-order rate is not easy because of the lack data and because the model uses a bulk rate (i.e., the effective rate should model degradation inside a numerical cell volume with primarily aerobic zones and only small volumes of microenvironments). The only source of information we could find is the study by Cook et al. (1995), who estimated rates of 5 to 40 $\times$ 10^{-4} d^{-1} in a groundwater aquifer with sudden depletion of O_2.

Engesgaard et al. (1996) found a longitudinal dispersivity of approximately α_L = 1 m by matching an analytical solution to three observed tritium profiles in the unsaturated zone at the Rabis Creek study site. The analytical solution assumed that flow was steady over the considered time period of 1961 through 1970. The dispersive effects from nonsteady flow were incorporated in the calibrated value of α_L. The α_L value of 1 m must be an upper bound, and a lower α_L is expected.

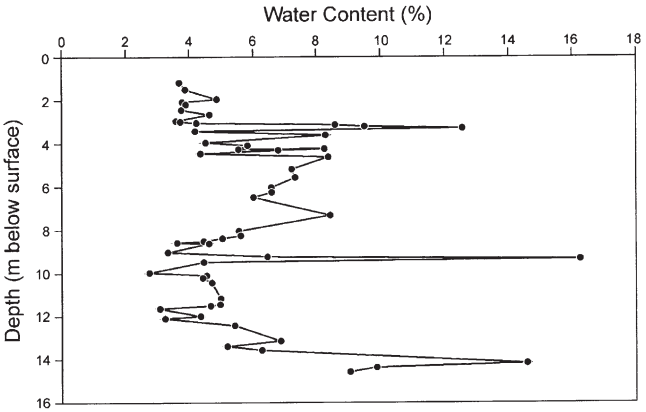

Fig. 3. Measured water content in the unsaturated zone (June 1995). The mean water content is approximately 6%.

RESULTS

Water Content

The measured volumetric water content (June 1995) is shown in Fig. 3. Average total porosity was measured to 0.39. The average water content at this time of year is approximately 6%, but varies between 3 and 16%. It is not possible to compare our numerical simulations of the flow dynamics with the observed water-content profile because not enough data are available to adequately characterize the hydraulic properties of the soil. Numerical results of the daily depth-averaged water content and yearly infiltration rate (at a depth of 1 m) are shown in Fig. 4. Infiltration varied appreciably with time, with a below average infiltration of 387 mm yr^{-1} in 1961 through 1979 and an above average infiltration of 507 mm yr^{-1} during 1980 through 1995. The mid 1970s in particular were dry, with yearly infiltration rates <300 mm yr^{-1}. The depth-averaged water content varied much less, between 9 and 12%. The average, over time, is approximately 0.1. This average is in reasonable agree-

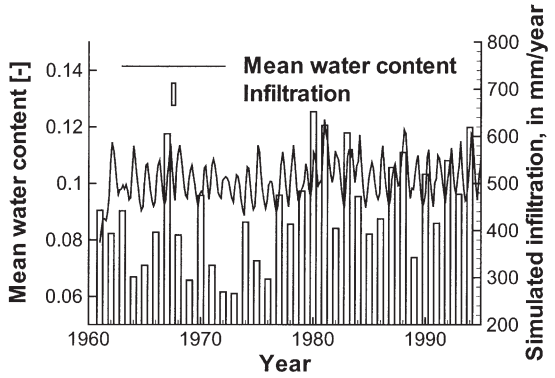

Fig. 4. Simulated results for daily depth-averaged water content and yearly infiltration rate.

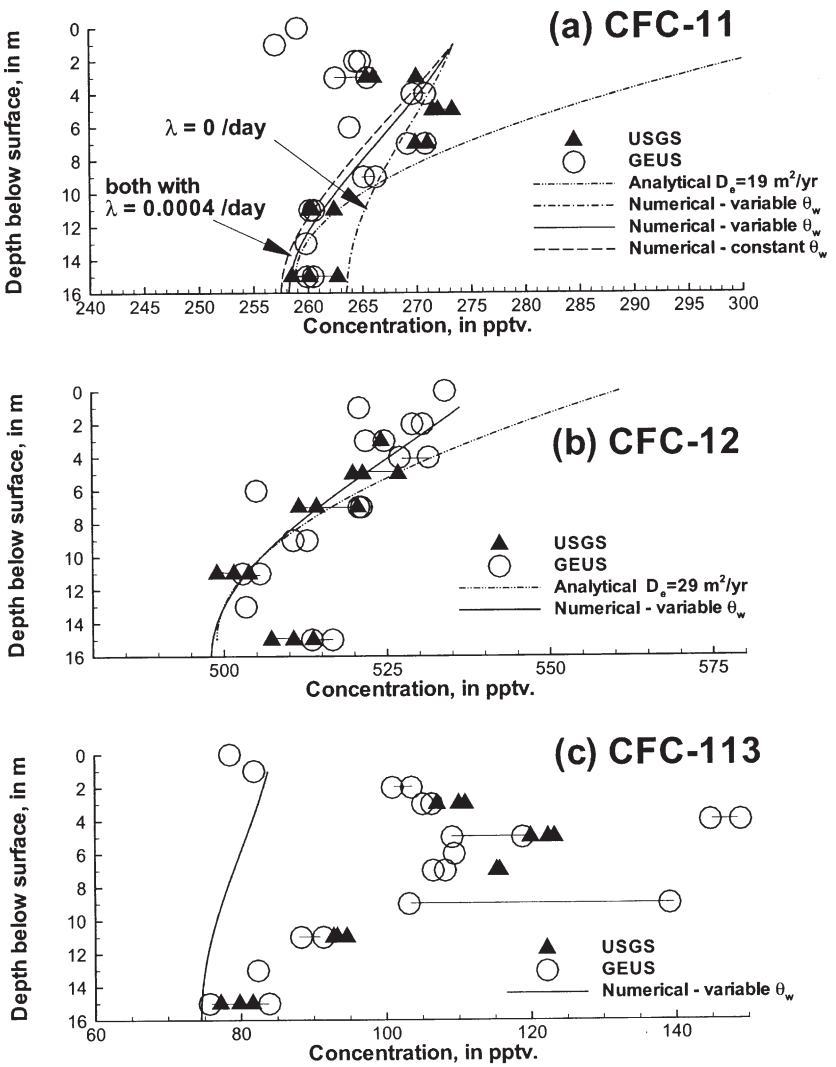

Fig. 5. Measured and simulated distributions of CFCs in the unsaturated zone. Note the small range in concentration scale. Horizontal lines connect replicate analyses of separate ampoules.

ment with monthly measurements from 1966 through 1967 (Andersen and Sevel, 1974). However, note that the simulation is not able to match the observed low mean water content of about 6% in June 1995 (Fig. 3).

CFC Profiles

The measured concentrations of the three CFC gases in the unsaturated zone air are shown in Fig. 5. Most of the samples were analyzed in duplicate. The differences between the two sets of measurements may be explained by the differences in time of sampling and slightly different sampling procedures. The CFC-113 concentrations are higher than the atmospheric concentrations observed at any time, indicating CFC-113 contamination. Presently, we cannot explain the source of contamination and are unable to match the observed profile with our choice of input function.

The concentrations of all three CFCs vary little with depth: ≈5% for CFC-11 and CFC-12 and ≈20% for CFC-113. The uniform concentration profiles indicate that an efficient mixing takes place in the unsaturated zone. However, a noticeable peak is present in the concentration profiles for CFC-11 in the upper 7 m of the profile, indicating instead that the rather uniform unsaturated zone profiles are a result of the recent stagnation and turnover of the atmospheric input functions (Fig. 2).

A comparison between numerically calibrated (based on nonsteady flow and thus variable θ_w) and observed CFC profiles is shown in Fig. 5. Transport of CFC-12 was simulated first because it was expected that CFC-12 would be less affected by sorption and degradation. With no degradation and sorption for CFC-12 a tortuosity coefficient of $\tau = 0.10$ was found. This value was used for CFC-11 and CFC-113 as well. For all gases, the best match to the observations was obtained for $\alpha_L = 0.05$ m. This value is less than the 1 m found by Engesgaard et al. (1996), which partly can be explained by inclusion of nonsteady flow. However, the simulations showed a lack of sensitivity to changes in α_L because of the nature of the atmospheric input function, with a linear increase in concentrations up to the early 1990s.

Figure 5a shows the simulated profile for CFC-11

assuming no sorption and with and without degradation in the bottom 4 m (where methane was observed). A good match to the observations below a depth of 5 m was obtained with a λ of 0.0004 d^{-1}, while assuming no degradation predicts concentrations that are too high. This rate is a factor of 1 to 10 less than that found by Cook et al. (1995). The difference may be explained by the coexistence of aerobic and anaerobic microenvironments. The rate is equivalent to a half-life of about 5 yr. Notice that the simulated profile is affected over the whole thickness of the unsaturated zone, even though degradation only occurs in the bottom 4 m. This is because degradation only takes place in the aqueous phase, which causes a transfer of CFC-11 from the air to the aqueous phase in the bottom 4 m and, consequently, then an increased diffusion from top to bottom. An almost similar fit can be obtained by neglecting degradation and instead allowing CFC-11 to sorb to the soil matrix with a $K_d = 0.06$. This K_d value is higher than the theoretical K_d value. Given our observations, especially with the small changes in CFC-11 concentrations, we are not able to conclusively say if sorption or degradation affects CFC-11 transport. The simulated concentrations are higher than observed in the upper 5 m. This difference can be explained by the atmospheric input function (Fig. 2a), where the leveling off and decline in concentration began around 1992 to 1996. The simulation, therefore, is sensitive to the choice of input function. The input function from Adrigole/Macehead, Ireland levels off too early, whereas the input function from Colorado, USA, used in the simulation, levels off too late.

For CFC-12, a good match to the observed profile was obtained assuming no sorption or degradation (Fig. 5b). The fit between the simulation and observation for CFC-12 is better than that for CFC-11 mainly because of less uncertainty in the input function (Fig. 2b). However, the observations in the top 3 m indicate that the leveling off in atmospheric CFC-12 concentrations started earlier than used in the input function. The observation at $z = 15$ m is higher than predicted by the model. The K_d value for CFC-113 also was chosen to be zero.

Periodically wetting and drying of the soil leads to variable air- and water-filled pore space fractions and, thus, to varying pore water velocities. The effect of changes in the water content will be greatest for the more soluble CFC-11 gas. Therefore, simulated CFC-11 concentration profiles based on steady and nonsteady flow, respectively, may give different results. A simulation with steady flow using the long-term mean infiltration of $q_w = 439$ mm yr^{-1} and $\bar{\theta}_w = 0.1$ is shown in Fig. 5a. Sorption was not included, but CFC-11 was allowed to degrade with the same rate as in the simulation with nonsteady flow. The maximum difference in concentration (at the water table) is <2 pptv.

Based on the results described above, it seems appropriate to test the simple analytical models for diffusion in soil air. For CFC-11, the simulated concentration in the gas phase at the water table in September 1995 was 260 pptv (Fig. 5a). This concentration corresponds to an atmospheric concentration in January 1989. Thus the soil gas appears to be 6.5 yr old if dated with CFC-11. Cook and Solomon (1995) defined these 6.5 yr as the "apparent time-lag" for the unsaturated zone. The period of linear increase in atmospheric concentrations starts in 1975 (with a start concentration of $c_0 = 115$ pptv) and ends in approximately 1991 (Fig. 2a). The rate of linear increase is estimated to be $k_l = 9.3$ pptv yr^{-1}, which gives a (synthetic) initial time of linear increase from zero concentration at approximately $t_0 = 1962$. The numerically computed time lag of 6.5 yr indicates that the observations closest to the water table are from the end of the linear growth phase. The ratio $D_e = D^*/\theta^*$ in Eq. [11] thus is calibrated to match the bottom of the profile (1–2 data points closest to the water table). The results of the analytical solution also are shown in Fig. 5a, using $D_e = 19$ m^2 yr^{-1}. This estimate can be compared with the results from the numerical analysis using Eq. [5] and [6], if $q_a = q_w = 0$ is assumed. The flow solution gave $\bar{\theta}_w = 0.10$, and using $\rho_b = 1.8$, $\tau = 0.10$, $K_d = 0.0$, and data from Table 1, a value of $D_e = 21.7$ m^2 yr^{-1} is obtained, close to the result of the analytical calibration. Using Eq. [14] and $D_e = 19$ m^2 yr^{-1}, $t_L^l = 5.2$ yr is obtained. The time lag is lower than the apparent time lag of 6.5 yr, which is because degradation or sorption is not included in the estimation. If we choose to use a K_d of 0.06, then $D_e = 18.50$ and $t_L^l = 6.1$ yr.

The analytical solution overestimates the observed concentrations of CFC-11 (Fig. 5a). The leveling off in the CFC-11 atmospheric input function and even the decrease are therefore seen in the observed profile. The numerically simulated profile better matches the observed profile, but the actual decrease in concentrations may have happened slightly earlier than simulated.

For CFC-12, a reasonable fit of the analytical solution to the lower half of the unsaturated zone results (Fig. 5b). The analytical solution was fitted to a larger part of the observed profile, because the trend with a linear increase in atmospheric concentrations continues 2 yr longer than for CFC-11, and the leveling off is much less pronounced. Also, the onset of the linear phase is estimated from Fig. 2b to be in 1971 (at a concentration of 143 pptv). The start of the linear increase in the model is set at $t_0 = 1961$ using a linear rate of increase of 16.0 pptv yr^{-1}. The fitted D_e of 29 m^2 yr^{-1} is similar to the 28 m^2 yr^{-1} calculated on the basis of Eq. [5] and [6]. The analytically estimated time lag is 3.9 yr, whereas the apparent time lag based on the observed concentration at the water table is approximately 4.3 yr.

The simulated CFC-113 profile is shown in Fig. 5c. Clearly, the high concentrations at depths of 3 to 9 m cannot be simulated with the model. We suspect that this may be caused by contamination during sampling or by an unknown local source. Thus, analytical modeling has not been pursued.

Input of CFC to Groundwater

The atmospheric and numerically simulated recharge input functions in the air phase at the groundwater table

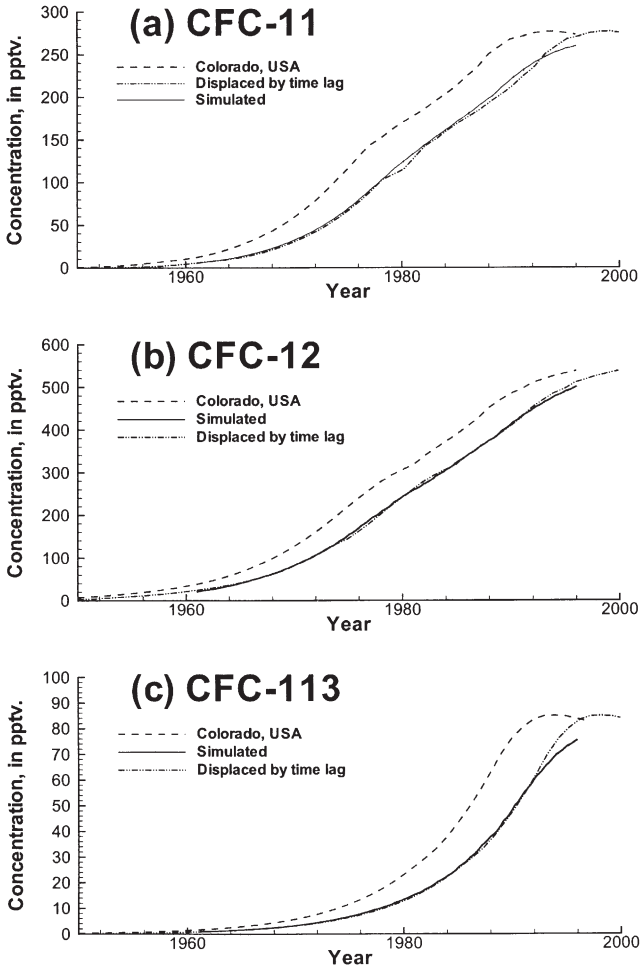

Fig. 6. Simulated (numerical as solid line and displaced by time lag as solid-dot) CFC concentrations at the water table beneath a 16-m-thick unsaturated zone at the Rabis Creek site compared with atmospheric concentrations (Colorado, USA).

for all three gases are shown in Fig. 6. The smaller apparent time lag for CFC-12 is a result of the higher rate of increase in the atmospheric input function (the slope of linear growth being 16 pptv yr^{-1} compared with 9.3 pptv yr^{-1} for CFC-11) leading to a higher concentration gradient. CFC-113 concentrations differ from the two other gases during the exponential growth period, which continues to 1985. The input function, therefore, has a linear growth period of only 5 yr (to 1990) before the growth rate decreases.

Figure 6 also shows a plot of the simulated input of CFCs to groundwater derived by displacing the atmospheric function by the analytically derived time lags during the exponential and linear growth phases, Eq. [9] and [14]. The analytical estimates of D_e were used. For CFC-113, we estimated D_e from Eq. [5] and [6] and shifted the atmospheric curve with the time lag for the exponential phase only. For the exponential growth phase, k_e is found as 0.15, 0.13, and 0.13 yr^{-1} for CFC-11 (ending in 1975), CFC-12 (ending in 1971), and CFC-113 (ending in 1985), respectively. The k_l growth rates are as given before. The time lags are given in Table 2.

The displaced input function for CFC-11 shows a longer time lag than the numerically simulated time lag for times <1990. For example, the time lags for the 1983 atmospheric concentration show a 0.5-yr longer time lag, which is 10% more than the numerically simulated time lag of 4.7 yr. For CFC-12 and CFC-113, shifting the atmospheric input function with a period equal to the analytically calculated time lags results in a groundwater input function that matches well with the numerically simulated up to about the early 1990s (Fig. 6). Dating water infiltrated later than early 1990s requires numerical simulations for CFC-11 and CFC-12 because the time lag cannot be assumed constant. For CFC-113, only water infiltrated earlier than the late 1980s may be assumed to have a constant time lag.

Table 2. Time lags for exponential and linear increases in atmospheric CFC concentrations at Rabis Creek. The linear period is from 1975 to 1991 (CFC-11), 1971 to 1993 (CFC-12), and 1985 to 1990 (CFC-113). The time lags are calculated from the analytical models.

	Time lags		
Model	CFC-11	CFC-12	CFC-113
	yr		
Exponential	4.8	3.6	3.8
Linear	5.2†–6.1‡	3.9	na§

† CFC-11 is conservative.
‡ K_d = 0.06 is applied.
§ Not applicable.

Sensitivity Study

Figure 7 shows the results of changing the infiltration rate on the CFC-11 time lag for two water contents (0.1 and 0.15). All other parameters are the same as before. The infiltration rate, q_w, was varied between 0 and 600 mm yr^{-1}. Thus, it was assumed that the water content was the same at all infiltration rates. The time lag was calculated for the 1983 atmospheric concentration. For reference, the time lags calculated with the fully dynamic model and the analytical solution [14] also are shown. The case of $\bar{\theta}_w$ = 0.10, which corresponds to the Rabis Creek conditions, is first discussed. Ideally, the numerical model simulation should match the analytical solution for q_w = 0. However, there is a difference of 0.1 yr, which is explained from differences in the upper boundary condition in the two solutions. The numerical model uses the observed atmospheric input function, whereas the analytical model uses an exact linear input. The difference of 0.1 yr represents the uncertainty in assuming a linear increase and estimating k_l from the atmospheric curve. For q_w = 439 mm yr^{-1} (long-term average), the difference is 0.05 yr between the computed time lags using steady and nonsteady flow. This result was also shown in Fig. 5a. The infiltration rate was higher (≈500 mm yr^{-1}) than the average in the period 1980 to 1995, Fig. 4. If 500 mm yr^{-1} is used, there is no difference between the calculated time lag using steady or nonsteady flow simulations. In the range 0 to 600 mm yr^{-1}, the difference in time lag always is less than half a year; thus, flow has had little effect on the historical input of CFC-11 to groundwater. Also, the analytical estimate of time lag is adequate for displacing the atmospheric

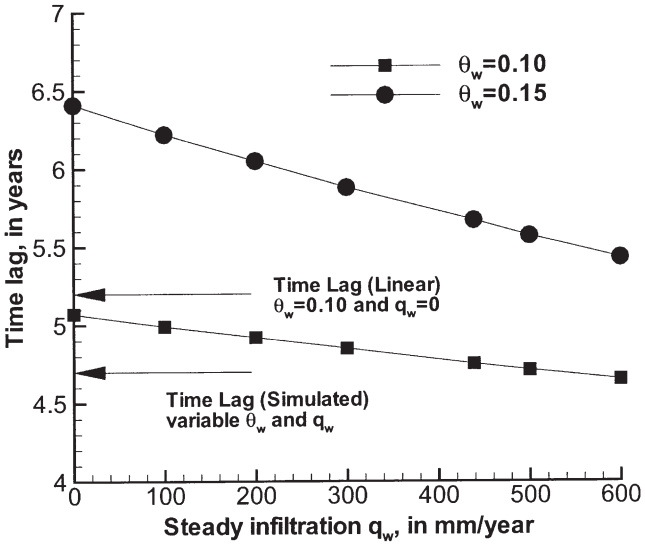

Fig. 7. Simulated time lag for 1983 atmospheric CFC-11 concentration as a function of steady infiltration q_w. Two cases of constant water content are shown: θ_w = 0.1 and 0.15. The corresponding simulated time lag for nonsteady infiltration is 4.7 yr. The analytical time lag under linear atmospheric increase in concentration is 5.2 yr.

input function because the difference between the two is only 0.5 yr. If the unsaturated zone is thicker than 15 m, then the decrease in time lag by including water flow still may be a small fraction of the total time lag. However, this decrease may be so large that it must be taken into account when predicting the historical input to groundwater. The effects discussed here are less for CFC-12 and CFC-113 because these gases are less soluble than CFC-11. Water flow, however, becomes more important at water content of 0.15. Zero infiltration gives a time lag of 6.4 yr. Infiltration rates need to be >600 mm yr^{-1} to reduce the time lag by more than 1 yr.

Thus, the analytical solutions are applicable for a broad range of conditions. A limited sensitivity analysis with the two analytical solutions Eq. [9] and [14] was performed to demonstrate when a lag time in the unsaturated zone becomes important. The time lags were only computed for CFC-11 and CFC-12 because they are representative for a range of self-diffusion coefficients and Henry's constants. We chose to focus the sensitivity analysis on the effects of changing the water content (0.05–0.15), the tortuosity coefficient (τ = 0.10 and 0.36), and the depth of the unsaturated zone (5–50 m). τ = 0.10 is equal to the calibrated value for Rabis Creek, whereas τ = 0.36 is calculated from the expression proposed by (Millington, 1959), $\tau = \theta_a^{7/3}/\theta^2$, where θ is the total porosity (0.39) and θ_a is calculated as $\theta - \bar{\theta}_w$ with $\bar{\theta}_w$ = 0.1. K_d = 0.06 was assumed for CFC-11, whereas CFC-12 was nonsorptive. No degradation was included.

The analytically computed time lags for three depths (5, 15, and 50 m), with two different tortuosity coefficients during the phases of linear and exponential increase in atmospheric concentrations are shown in Fig. 8. If the unsaturated zone is shallow, L = 5 m, then the time lag is very small (<1 yr) for both gases. Because the linear phase ended in approximately 1991 and 1993 for CFC-11 and CFC-12, respectively, this means that data must be from before approximately 1992 or 1994 for the analytical solutions to apply.

The case with L = 15 m, $\bar{\theta}_w$ = 0.10, and τ = 0.10 corresponds to the conditions at the Rabis Creek site (assuming $q_a = q_w = 0$), which shows time lags >1 yr. The time lags in the linear phase for CFC-11 and CFC-12 were calculated to 5.2 to 6.1 and 3.9 yr, respectively (Table 2). Sampling after 1998, therefore, would not detect this period, and the analytical solution would not apply.

The time lag is important for larger depths ($L \geq 50$ m). In the case of τ = 0.1 and a water content of 0.15, the time lag for CFCs after the start of the linear phase (early to mid 1970s) is about 50 (CFC-12) and 80 (CFC-11) years. CFCs from after the mid 1970s can likely be found in 50-m-deep unsaturated zones. In the exponential phase the time lags are 20 to 30 yr. The time lags in the two different phases now are different, about 30 to 50 yr. In reality, there will be a much smoother transition in the time lag. So although the calculated time lags of the exponential phase indicate that sampling today would not detect this phase, it is likely that a 50-m-deep unsaturated zone would be a mixture of CFC gases from both the linear and exponential phases. This would make it difficult to use the analytical approach. For the case of τ = 0.36, sampling today only would detect the linear phase for CFC-11 because the time lags for the other cases are about 10 yr and the linear phase ended more than 10 yr ago.

The time lags for CFC-11 are higher and more variable than for CFC-12 (and CFC-113) because of CFC-11's higher solubility. One of the greatest uncertainties in estimating time lag is associated with the tortuosity coefficient. For the linear phase, the time lag scales linearly with the inverse of the tortuosity coefficient (see Eq. [14]). In our study and the studies by Weeks et al. (1982) and Busenberg et al. (1993), the tortuosity coefficient has been a fitting parameter. It is difficult to estimate this parameter independently except for well-defined conditions, such as in the sand dunes investigated by Severinghaus et al. (1997). These dry sand dunes were 70 m deep, receiving about 50 mm yr^{-1} precipitation. They found that diffusion model results with a tortuosity coefficient of 0.6 for a dry soil (uncalibrated; see Millington [1959] and Weeks et al. [1982]) fitted observed CFC profiles. Another case where a relatively high tortuosity coefficient was found was reported by Oster et al. (1996). The forest soil was described as well aerated, which could explain the high effective diffusion coefficient (we estimate τ = 0.44 on the basis of the effective diffusion coefficient). In the general case, the tortuosity coefficient will be a complex function of time-dependent changes in water content, pore connectivity, and other physical properties of the soil.

CONCLUSIONS

A numerical model was used to simulate observed CFC gas profiles in the 16-m-thick unsaturated zone at Rabis Creek, Denmark. A low tortuosity coefficient of τ = 0.1 was fitted to the observed profiles. CFC-11 was

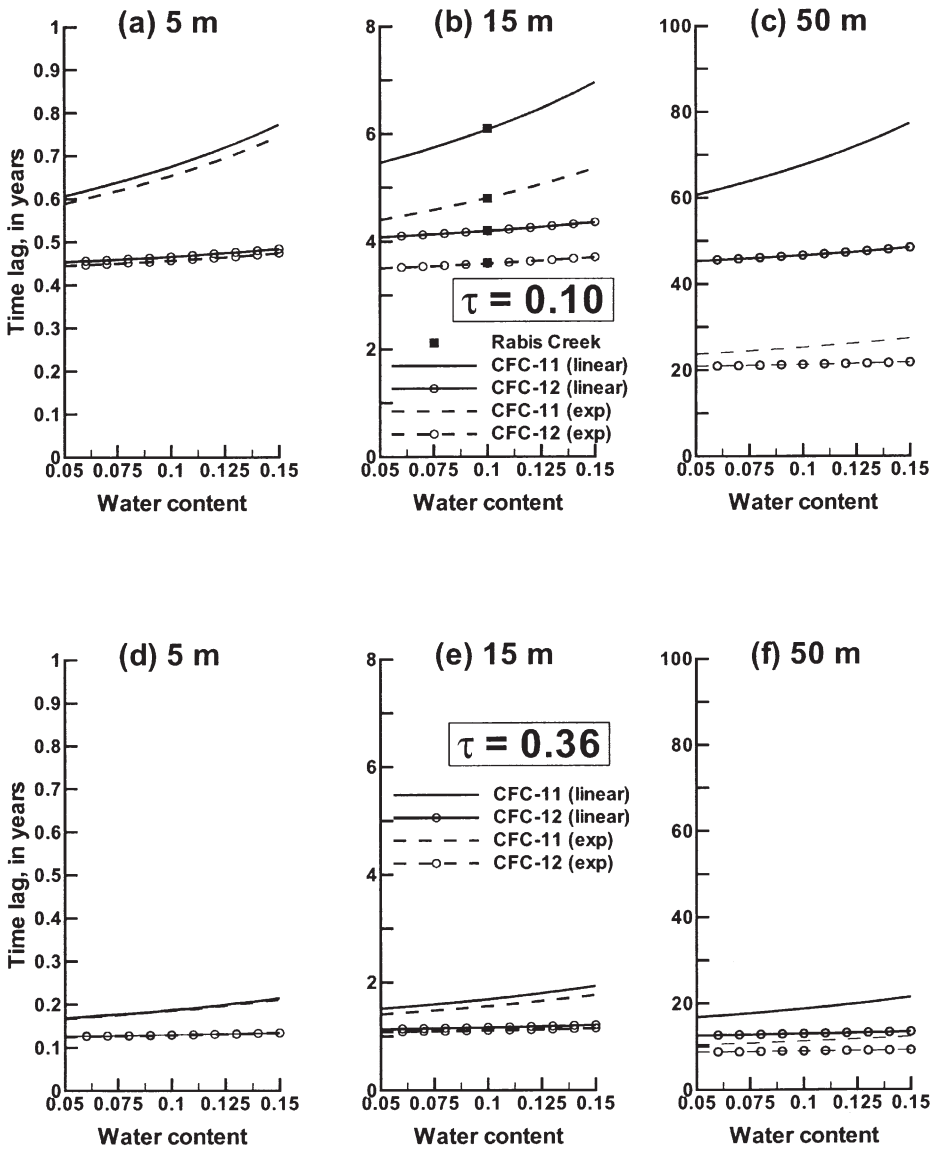

Fig. 8. Effect of water content, depth of unsaturated zone, and tortuosity coefficient on calculated time lags for CFC-11 and CFC-12 during exponential and linear increase in atmospheric concentrations. (a–c) τ = 0.1; (d–f) τ = 0.36.

shown to be slightly affected by either degradation or sorption, whereas CFC-12 and CFC-113 were found to move conservatively through the unsaturated zone. Degradation of CFC-11, with a first-order rate of 0.0004 d^{-1}, in the bottom 4 m is likely because of the presence of methane at these depths. The degradation rate corresponds to a half-life of 5 yr in the bottom 4 m. In comparison, the time lag in air is 5.2 to 6.1 yr for the 15-m-thick unsaturated zone. Sorption of CFC-11, however, was modeled with a high K_d value of 0.06, which was not expected due to the very low organic content.

Analytical models for diffusion and time lags were adapted from Cook and Solomon (1995) for the case of exponential increase and from Carslaw and Jaeger (1959) for linear increase in atmospheric CFC concentrations. The model for linear increase was fitted to CFC-11 and CFC-12 profiles in the lower part of the profile, providing an estimate of the effective diffusion coefficient. The analytical solutions agreed well with the numerical solution.

For the conditions at the Rabis Creek field site, the results show that it is possible to neglect water flow when quantifying transport of the three gases through the unsaturated zone. For the most soluble gas, CFC-11, the error in the calculated time lag is on the order of 1 yr, when neglecting water flow. For CFC-12 and CFC-113 the error is less than for CFC-11. The analytically derived time lags will suffice to displace the atmospheric input function by fixed time lags to predict the historical input to groundwater. However, water flow becomes important at a mean water content of 0.15 and infiltration rates >400 mm yr^{-1}.

A sensitivity analysis using the analytical models demonstrates the importance of the depth of the unsaturated zone, the water content, and tortuosity coefficient on the estimated time lag. The most critical parameter is

the tortuosity coefficient. For the model with a linear increase, the time lag scales inversely with tortuosity coefficient. High tortuosity coefficients ($\tau = 0.36$) mean that only the linear phase can be found today in deep (>20 m) unsaturated zones. The analytical solution presented in this work (Eq. [14]) for the linear phase then may apply. Low tortuosity coefficients ($\tau = 0.10$) result in a large difference in time lags in the linear and exponential phases (30–50 yr), which is not realistic. It is, therefore, difficult to predict if, for example, gas concentrations from the exponential phase are no longer present in the a deep unsaturated zone or whether a gas profile is a mixture of concentrations from both the linear and exponential phases. The use of analytical methods is therefore questionable. Numerical simulations may be an option, as described in our work, but only for conditions where, for example, barometric pumping of air through fractures or gross heterogeneity in transport properties are not present.

APPENDIX

c_w concentration of gas dissolved in water (moles per gram of water)
c_a concentration of gas in air (moles per cubic centimeter of gas)
c_0 initial concentration of gas in air (moles per cubic centimeter of gas)
D_w dispersion coefficient (square meters per year)
D_a $= \tau D_{CFC}$, CFC gas diffusion coefficient (square meters per year)
D^* bulk diffusion coefficient (square meters per year)
D_e effective diffusion coefficient (square meters per year)
D_{CFC} self-diffusion coefficient for a CFC gas into atmospheric air (square meters per year)
f_{oc} soil organic content (grams of C per gram of solid)
k_e rate of exponential increase in the atmospheric CFC function (per year)
k_l rate of linear increase in the atmospheric CFC function (pptv per year)
K_d solid–water distribution coefficient (grams of water per gram of solid)
K_{wa} water–air partitioning coefficient (cubic centimeters gas per gram water)
K_{oc} octanol–water distribution coefficient (grams of water per gram of C)
L depth of unsaturated zone (meters)
R $= 1 + \rho_b/(\rho_w\theta_w)K_d$ (no unit)
q_w Darcy flux (cubic meters of water per year per square meter)
$\overline{q}_w$ mean Darcy velocity (cubic meters of water per year per square meter)
q_a advective flux of air (cubic meters of gas per year per square meter)
$\overline{q}_a$ mean advective flux of air (cubic meter of gas per year per square meter)
q^* bulk advective flux of air (cubic meters of gas per year per square meter)
t time (years)
t_L^e time lag for the exponential phase (years)
t_L^l time lag for the linear phase (years)
t_0 initial time for start of CFC release (years)
v_w pore water velocity (cubic meters of water per year per square meter)
z depth oriented positive downwards (meters)
α_L longitudinal dispersivity (meters)
ρ_w water density (grams per cubic centimeter of water)
ρ_b bulk density of the media (grams per cubic centimeter)
θ total porosity (cubic centimeters of porous medium per cubic centimeter)
θ_w volumetric water content (cubic centimeters of water per cubic centimeter)
$\overline{\theta}_w$ mean volumetric water content (cubic centimeters of water per cubic centimeter)
θ_a volumetric air content (cubic centimeters of gas per cubic centimeter)
θ^* averaged volumetric air content (cubic centimeters of air per cubic centimeter)
τ tortuosity of the porous media (no unit)
λ first-order degradation rate (per day)

ACKNOWLEDGMENTS

The Danish Environmental Research Program and the Geological Survey of Denmark and Greenland supported this study. Two Master's thesis students, Kamilla G. Nielsen and Bjarke Ørbeck, who are greatly acknowledged for their work, carried out an early part of this work. Søren Nielsen, Geological Survey of Denmark and Greenland, is acknowledged for his valuable assistance in the field. The authors also would like to thank three anonymous reviewers for their insightful and helpful comments.

REFERENCES

Andersen, L.J., and T. Sevel. 1974. Six years environmental tritium profiles in the unsaturated and saturated zones, Grønhøj, Denmark. p. 3–20. *In* Proceedings Series: Isotope Techniques in Groundwater Hydrology. Vol. I. Rep. IAEA-SM-1182/1.

Böhlke, J.K., and J.M. Denver. 1995. Combined use of groundwater dating, chemical, and isotopic analyses to resolve the history and fate of nitrate contamination in two agricultural watersheds, Atlantic coastal plain, Maryland. Water Resour. Res. 31:2319–2339.

Bu, X., and M.J. Warner. 1995. Solubility of chlorofluorocarbon 113 in water and seawater. Deep Sea Res. 42:1151–1161.

Busenberg, E., and L.N. Plummer. 1992. Use of chlorofluorocarbons (CCl_3F and CCl_2F_2) as hydrologic tracers and age-dating tools: The alluvium and terrace system of central Oklahoma. Water Resour. Res. 28:2257–2287.

Busenberg, E., and L.N. Plummer. 2000. Dating young groundwater with sulfur hexafluoride: Natural and anthropogenic sources of hexafluoride. Water Resour. Res. 36:3011–3030.

Busenberg, E., E.D. Weeks, L.N. Plummer, and R.C. Bartholomay. 1993. Age dating ground water by use of chlorofluorocarbons (CCl_3F and CCl_2F_2), and distribution of chloroflurocarbons in the unsaturated zone, Snake River plain aquifer, Idaho National Engineering Laboratory, Idaho. Water-Resources Investigations Rep. 93-4054. U.S. Geological Survey, Denver, CO.

Carslaw, H.S., and J.C. Jaeger. 1959. Conduction of heat in solids. Oxford University Press, Oxford, UK.

Ciccioli, P., W.T. Cooper, P.M. Hammer, and J.M. Hayes. 1980. Organic solute-mineral surface interactions: A new method for the determination of groundwater velocities. Water Resour. Res. 16: 217–223.

Cook, P.G., and D.K. Solomon. 1995. Transport of atmospheric trace gases to the water table: Implications for groundwater dating with chlorofluorocarbons and Krypton 85. Water Resour. Res. 31:263–270.

Cook, P.G., D.K. Solomon, L.N. Plummer, E. Busenberg, and S.L. Schiff. 1995. Chlorofluorocarbons as tracers of groundwater transport processes in shallow, silty sand aquifer. Water Resour. Res. 31:425–434.

Cook, P.G., D.K. Solomon, W.E. Sanford, E. Busenberg, L.N. Plummer, and R.J. Poreda. 1996. Inferring shallow groundwater flow in saprolite and fractured rock using environmental tracers. Water Resour. Res. 32:1501–1509.

Ekwurzel, B., P. Schlosser, W.M.S. Jr, L.N. Plummer, E. Busenberg, R.L. Michel, R. Weppernig, and M. Stute. 1994. Dating of shallow

groundwater: Comparison of the transient tracers $^{3}H/^{3}He$, chlorofluorocarbons, and ^{85}Kr. Water Resour. Res. 30:1693–1708.
Engesgaard, P., K.H. Jensen, J.W. Molson, E.O. Frind, and H. Olsen. 1996. Large-scale dispersion in a sandy aquifer: Simulation of subsurface transport of environmental tritium. Water Resour. Res. 32:3253–3266.
Happell, J.D., R.M. Price, Z.T. Top, and P.K. Swart. 2003. Evidence for the removal of CFC-11, CFC-12, and CFC-113 at the groundwater-surface water interface in the Everglades. J. Hydrol. (Amsterdam) 279:94–105.
Johnston, C.T., P.G. Cook, S.K. Frape, L.N. Plummer, E. Busenberg, and R.J. Blackport. 1998. Ground water age and nitrate distribution within a glacial aquifer beneath a thick unsaturated zone. Ground Water 36:171–180.
Katz, B.G., T.M. Lee, L.N. Plummer, and E. Busenberg. 1995. Chemical evolution of groundwater near a sinkhole lake, northern Florida. 1. Flow patterns, age of groundwater, and influence of lake water recharge. Water Resour. Res. 31:1549–1564.
Kimball, B.A., and E.R. Lemon. 1972. Theory of soil air movement due to pressure fluctuations. Agric. Meteorol. 9:163–181.
Massmann, J., and D.F. Farrier. 1992. Effects of atmospheric pressures on gas transport in the vadose zone. Water Resour. Res. 28:777–791.
Millington, R.J. 1959. Gas diffusion in porous media. Science 130: 100–102.
Nielsen, K.G., and B.D. Ørbeck. 1995. Use of tracers for groundwater age dating, Case study: The use of CFC to age date groundwater at Rabis Creek. (*In* Danish.) M.S. thesis. Department of Hydrodynamics and Water Resources (ISVA), Technical University of Denmark, Lyngby.
Nilson, R.H., E.W. Peterson, K.H. Lee, N.R. Burkhard, and J.R. Hearst. 1991. Atmospheric pumping: A mechanism causing vertical transport of contaminated gases through fractured permeable media. J. Geophys. Res. 96(B13):21933–21948.
Olsen, H., C. Ploug, U. Nielsen, and K. Sørensen. 1993. Reservoir characterization applying high-resolution seismic profiling, Rabis Creek, Denmark. Ground Water 31:84–90.
Oster, H., C. Sonntag, and K.O. Münnich. 1996. Groundwater age dating with chlorofluorocarbons. Water Resour. Res. 32:2989–3001.
Plummer, L.N., and E. Busenberg. 1999. Chlorofluorocarbons. Chapter 15. p. 441–478. P.G. Cook and A.L. Herczeg (ed.) Kluwer Academic Publishers, Boston.
Plummer, L.N., E. Busenberg, J.K. Böhlke, D.L. Nelms, R.L. Michel, and P. Schlosser. 2001. Groundwater residence times in Shenandoah National Park, Blue Ridge Mountains, Virginia, USA: A multitracer approach. Chem. Geol. 179:93–111.
Plummer, L.N., M.G. Rupert, E. Busenberg, and P. Schlosser. 2000. Age of irrigation water in groundwater from the Eastern Snake river plain aquifer, South-Central Idaho. Ground Water 38:264–283.
Postma, D., C. Boesen, H. Kristiansen, and F. Larsen. 1991. Nitrate reduction in an unconfined sandy aquifer: Water chemistry, reduction processes, and geochemical modeling. Water Resour. Res. 27:2027–2045.
Prinn, R.G., R.F. Weiss, P.J. Fraser, P.G. Simmonds, D.M. Cunnold, F.N. Alyea, S. O'Doherty, P. Salameh, B.R. Miller, J. Huang, R.H.J. Wang, D.E. Hartley, C. Harth, L.P. Steele, G. Sturrock, P.M. Midgely, and A. McCulloch. 2000. A history of chemically and radiatively important gases in air deduced from ALE/GAGE/AGAGE. J. Geophys. Res. 105:17751–17792.
Reilly, T.E., L.N. Plummer, P.J. Phillips, and E. Busenberg. 1994. The use of simulation and multiple environmental tracers to quantify groundwater flow in a shallow aquifer. Water Resour. Res. 30:421–433.
Schwarzenbach, R.P., P.M. Gschwend, and D.M. Imboden. 1993. Environmental organic chemistry. John Wiley and Sons, New York.
Severinghaus, J.P., R.F. Keeling, B.R. Miller, R.F. Weiss, and B. Deck. 1997. Feasibility of using sand dunes as archives of old air. J. Geophys. Res. 102(D14):16783–16792.
Steefel, C.I., and K.T.B. MacQuarrie. 1996. Approaches to modeling of reactive transport in porous media. p. 83–129. *In* P.C. Lichtner et al. (ed.) Reactive transport in porous media. Reviews in Mineralogy 34. Mineralogical Society of America, Washington, DC.
Szabo, Z., D.E. Rice, L.N. Plummer, E. Busenberg, S. Drenkard, and P. Schlosser. 1996. Age dating of shallow groundwater with chlorofluorocarbons, tritium/helium 3, and flow path analysis, southern New Jersey coastal plain. Water Resour. Res. 32:1023–1038.
Thomas, R. (1982). Volatilization from soil. *In* W.J. Lyman et al. (ed.) Handbook of chemical properties estimation methods. McGraw-Hill, New York.
Thorstenson, D.C., E.P. Weeks, E.B.H. Haas, L.N. Plummer, and C.A. Peters. 1998. Chemistry of unsaturated zone gases sampled in open boreholes at the crest of Yucca Mountain, Nevada: Data and basic concepts of chemical and physical processes in the mountain. Water Resour. Res. 34:1507–1529.
Warner, M.J., and R.F. Weiss. 1985. Solubility of chlorofluorocarbons 11 and 12 in water and seawater. Deep Sea Res. 32:1485–1497.
Weeks, E.P., E.E. Douglas, and G.M. Thompson. 1982. Use of atmospheric fluorocarbons F-11 and F-12 to determine the diffusion parameters of the unsaturated zone in the southern high plains of Texas. Water Resour. Res. 18:1365–1378.